ROOM MODES IN RECTANGULAR ROOMS WITH COMPLEX IMPEDANCE BOUNDARIES

David Jun*[1,2], Josef Plasek[1], Monika Rychtarikova[2], Christ Glorieux[3]

*David.Jun@vut.cz
[1]Brno University of Technology, Faculty of Civil Engineering, Brno, Czech Republic
[2]KU Leuven, Department of Architecture, Campus Brussels and Ghent, Belgium
[3]KU Leuven, Department of Physics and Astronomy, Heverlee, Belgium

Abstract
In many calculation approaches in room acoustics, one models the reflection of surfaces via a positive, real absorption coefficient, neglecting the fact that the reflection coefficient can have a non-zero phase. For some sound-absorbing structures such as resonators, this simplification leads to erroneous results, e.g. when room modes are of interest.

This contribution presents an approach for the calculation of room mode frequencies in a rectangular room with complex and frequency-dependent acoustic impedance wall boundary conditions. The results are to be used for auralizations of different scenarios in which the modal behaviour of a room is modified, and for evaluation by listening tests.

Keywords
Complex acoustic impedance, analytical solution, room modes, resonators

1 INTRODUCTION

In room acoustics of small spaces, room modes are of interest. This is especially true in cases where music playing, music production or listening to music are parts of the programme [1]. Room modes are natural resonances of the space, which occur as standing waves. They are commonly associated only with room dimensions. This is a reasonable simplification in cases where the room boundaries are rigid or have a nearly real-valued pressure reflection factor. With this assumption, no phase shift of the reflection occurs at the boundary and the sound absorption coefficient can be effectively used for boundary definition, since it holds only the information about the pressure reflection factor amplitude.

Acoustic practitioners see this simplification applied in common calculation methods – in the well-known Sabine's formula for reverberation time calculations [2], but it is also used for image source (IS) and stochastic ray tracing (SRT) methods [3], [4]. These methods commonly do not allow to calculate modal behaviour of a space, and therefore incorporating possible phase shifts at the boundary is irrelevant for those approaches.

In contrast, in modelling small spaces at low frequencies (usually assumed to be below their Schroeder frequency), room modes occur quite isolated in frequency-wise manner, making their exact spectral shape and position important. This leads to the need for a more precise boundary condition representation. Since purely wave-based methods are computationally expensive for full audible spectrum calculations, some hybrid methods have been developed [5], [6]. Some structures commonly used for low-frequency damping, such as resonators, show highly complex behaviour, which, when simplified to the sound absorption coefficient, can lead to erroneous results.

Numerical and statistical room acoustic simulations are commonly used for auralizations and listening tests [7], [8], [9]. However, in cases where low frequencies and room modes are of interest, it is necessary to use one of the hybrid calculation methods. For these models, an analytical solution of the modal frequencies could be used as a validation tool.

A solution of a rectangular room with rigid and non-rigid symmetrical boundary conditions can be found in [10]. For non-rigid symmetrical boundaries, except for a 1D simplified geometry, a simple explicit equation for the modal behaviour cannot be derived. In the following, the solution from [10] is extended towards asymmetrical complex impedance boundary conditions. The problem is expressed and iteratively solved as a minimization problem of four equations, three for different directions and one for the general requirement (1)

$$k = \omega/c \tag{1}$$

where k, in m^{-1}, is the wavenumber, ω, in rad^{-1}, is the angular frequency and c, in m/s, is the speed of sound in air.

DOI 10.13164/juniorstav.2024.24121

2 METHODOLOGY

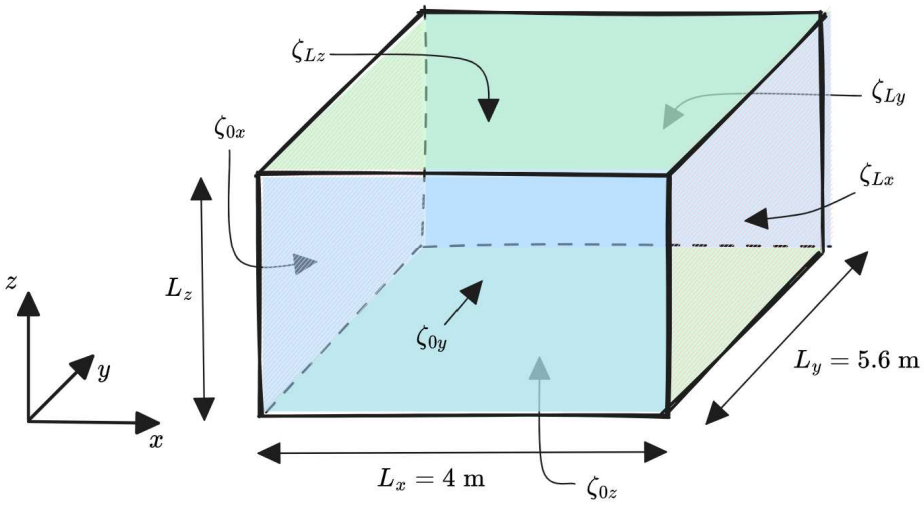

Fig. 1 Layout of the considered room and the boundary conditions.

Fig. 1 depicts the geometry of the considered rectangular room, for which we want to calculate the modes.We define the normalized surface impedance of wall surfaces ζ as:

$$\zeta = \frac{z_s}{z_c} \tag{2}$$

where z_s, in Pa.s.m^{-1}, is the acoustic impedance at the boundary and $z_c = \rho c$, in Pa.s.m^{-1}, is the characteristic impedance of air. ρ, in kg/m^3, is the density of air and c, in m/s, is the speed of sound propagation in air. The normalized surface impedance can be calculated from the pressure reflection factor as:

$$\zeta = \frac{1 + r}{1 - r} \tag{3}$$

The solution for asymmetrical impedance boundary conditions begins with the following boundary conditions for the x direction:

$$\zeta_{0x} \frac{\mathrm{d}p}{\mathrm{d}x} = \mathrm{i}kp \quad \text{for } x = 0 \tag{4}$$

$$\zeta_{Lx} \frac{\mathrm{d}p}{\mathrm{d}x} = -\mathrm{i}kp \quad \text{for } x = L_x \tag{5}$$

where ζ_{0x} and ζ_{Lx} are the normalized surface impedances of the wall surfaces at $x = 0$ and $x = L_x$ respectively, p, in Pa, is the acoustic pressure at these boundaries and k is the wavenumber. In this case, the general wave equation solution can be formulated as:

$$p(x) = p^+ \exp(-\mathrm{i}k_x x) + p^- \exp(\mathrm{i}k_x x) \tag{6}$$

where p is the total acoustic pressure and p^+ and p^- represent the acoustic pressure amplitudes of the acoustic waves travelling in the positive and negative x direction. Inserting this equation into the boundary conditions leads to the following set of equations:

$$p^+(k + k_x\zeta_{0x}) + p^-(k - k_x\zeta_{0x}) = 0 \tag{7}$$

$$p^+(k - k_x\zeta_{Lx}) + p^-(k + k_x\zeta_{Lx}) \exp(2\mathrm{i}k_x L_x) = 0 \tag{8}$$

To obtain a non-vanishing solution, the determinant of the coefficients needs to be zero:

$$\begin{vmatrix} (k + k_x\zeta_{0x}) & (k - k_x\zeta_{0x}) \\ (k - k_x\zeta_{Lx}) & (k + k_x\zeta_{Lx}) \exp(2\mathrm{i}k_x L_x) \end{vmatrix} = 0 \tag{9}$$

DOI 10.13164/juniorstav.2024.24121

This ultimately leads to the following condition that needs to be satisfied:

$$e^{2ik_xL_x} = \frac{(k - k_x\zeta_{0x})(k - k_x\zeta_{Lx})}{(k + k_x\zeta_{0x})(k + k_x\zeta_{Lx})} \tag{10}$$

A similar condition holds for the y and z directions, leading to three equations to be satisfied. The search for solutions for the angular frequency and the three wavenumbers satisfying the above equations, as well as the general wave propagation condition Eq. (1), can be performed by setting $\omega = ck = c\left(k_x^2 + k_y^2 + k_z^2\right)^{1/2}$ and minimizing the three quantities f_1, f_2 and f_3 by varying the three wavenumber components k_x, k_y and k_z in 3D:

$$f_1 = \left| e^{2ik_xL_x} - \frac{(k - k_x\zeta_{0x})(k - k_x\zeta_{Lx})}{(k + k_x\zeta_{0x})(k + k_x\zeta_{Lx})} \right|^2 \tag{11}$$

$$f_2 = \left| e^{2ik_yL_y} - \frac{(k - k_y\zeta_{0y})(k - k_y\zeta_{Ly})}{(k + k_y\zeta_{0y})(k + k_y\zeta_{Ly})} \right|^2 \tag{12}$$

$$f_3 = \left| e^{2ik_zL_z} - \frac{(k - k_z\zeta_{0z})(k - k_z\zeta_{Lz})}{(k + k_z\zeta_{0z})(k + k_z\zeta_{Lz})} \right|^2 \tag{13}$$

Note that although a minimum search can be performed for each value of the angular frequency, satisfactory solutions of Eqs. (11), (12), (13) are only expected for a discrete number of angular frequencies.

Alternatively, in addition to the three wavenumber components, also ω can be left free in the search, by also requiring that:

$$f_4 = \left| k_x^2 + k_y^2 + k_z^2 - \frac{\omega^2}{c^2} \right| \tag{14}$$

Note that the approach allows scenarios in which the impedances are complex and frequency-dependent.

3 RESULTS

In this work, without loss of generality, we illustrate the approach for axial modes, i.e., „1D“ modes of which only one of the k_x, k_y and k_z is non-zero. That is possible because the more complicated modes are composed of the same allowed sets of k_x, k_y and $k_z$values, fulfilling Eq. (1). For axial modes in each direction, the minimization problem simplifies to:

$$f_5 = \left| e^{2ik_xL_x} - \frac{(\omega/c - k_x\zeta_{0x})(\omega/c - k_x\zeta_{Lx})}{(\omega/c + k_x\zeta_{0x})(\omega/c + k_x\zeta_{Lx})} \right|^2 \tag{15}$$

In 1D, it can be shown how the direct solution of Eq. (10) holds for some special cases.For example, in the case of symmetrical boundary conditions, with $\zeta_{0x} = \zeta_{Lx} \gg 1$ and $\zeta_{0x} = \zeta_{Lx} \ll 1$, we obtain the following set of solutions:

$$k_x = n_x \frac{\pi}{L_x} \tag{16}$$

The assymetrical case $\zeta_{0x} \ll 1 \ll \zeta_{Lx}$ results in:

$$k_x = \left(n_x + \frac{1}{2}\right)\frac{\pi}{L_x} \tag{17}$$

This adequately reflects the acoustic pressure mimima on the boundary $x = 0$ and maxima on the other one $x = L_x$. The other asymmetrical case of $\zeta_{0x} \gg 1$ and $\zeta_{Lx} = i$, ζ_{0x} being purely real and ζ_{Lx} being purely imaginary, leads to the following solution:

$$k_x = \left(n_x + \frac{1}{4}\right)\frac{\pi}{L_x} \tag{18}$$

Adding an imaginary part (and thus non-zero phase) to a surface impedance obviously modifies the modes. Fig. 1 illustrates this effect for an axial mode in the x-direction. We have applied the Nelder-Mead simplex

DOI 10.13164/juniorstav.2024.24121

algorithm [11], [12], [13] for minimizing Eq. (15) near a mode with real surface impedances ($n_x = 2$) for different imaginary parts of ζ_{0x} and with $\zeta_{Lx} \gg 1$.

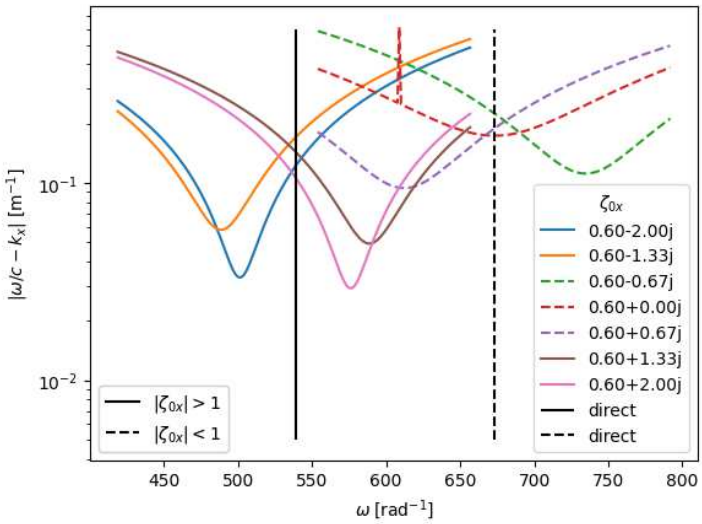

Fig. 2 Influence of a non-zero imaginary part on one of the room mode resonance frequencies.

As expected, the modal frequency deviates from the value for the case with a real impedance proportionally to the magnitude of the imaginary part. Adding a non-zero phase to the reflection coefficient can be seen as equivalent to changing the acoustic path length of the room along the propagation direction, and thus the effective dimension of the room along that direction.

The following example shows the results for a two-dimensional room with dimensions 4 × 5.6 m and frequency-independent boundary conditions: $\zeta_{0x} = \zeta_{0y} = \zeta_{Ly} = 10^3$, $\zeta_{Lx} = 0.5i$. The left panel of Fig. 2 shows that the minimization converges reasonably well. The solution enables extracting a set of possible k values for each direction.

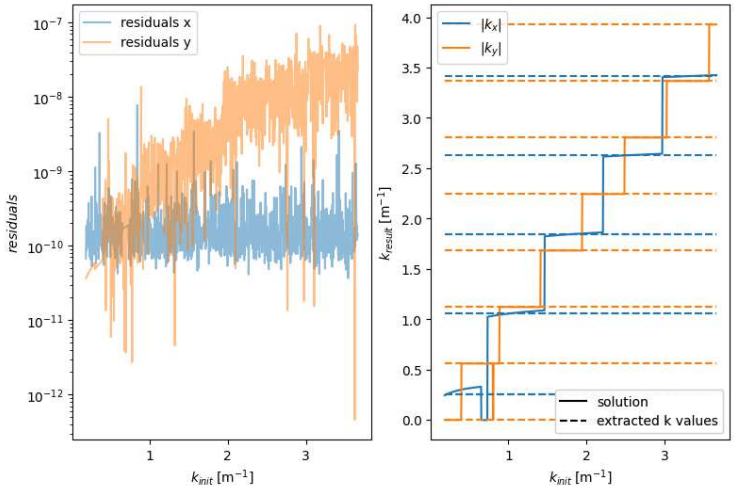

Fig. 3 Results of a wavenumber search in a 2D room situation. The left panel shows the final residuals of f_5 for each initial wavenumber $k_{init} = \omega/c$. The right panel shows the amplitude of the wavenumbers to which the minimization converged.

Fig. 4 shows the result of the 3D minimum search for the function:

$$f_6(k_x, k_y, \omega) = \left| k_x^2 + k_y^2 - \frac{\omega^2}{c^2} \right| / \omega \tag{19}$$

where k_x and k_y were restricted to the previously extracted values for two cases of non-rigid boundaries with the complex reflection factor amplitude $|r_{Lx}| = 0{,}9$ but different phases. The left panel shows the zero-phase reflection

DOI 10.13164/juniorstav.2024.24121

factor results, while the right panel shows the $\pi/3$ phase-shifted results. The crosses show the center of mass of $1/f_6$ local maxima regions.

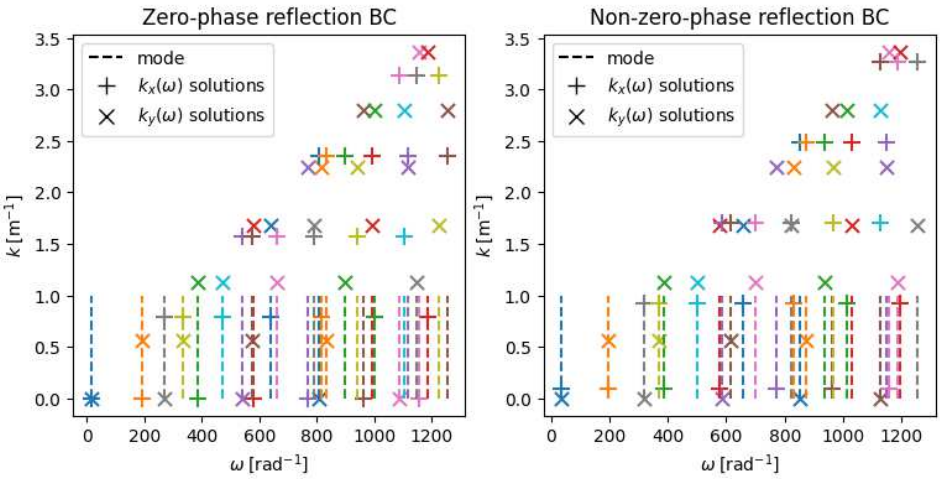

Fig. 4 Illustration of a 2D room mode search based on the previously extracted possible wavenumbers. Both cases share the same amplitude of the pressure reflection factor at the boundary $x = L_x$, but they are phase-shifted by $\pi/3$.

Fig. 5 shows a specific pair of modes for the previously calculated cases. These modes share their k_y value, whereas their k_x value is similar but slightly different. Fig. 5 nicely demonstrates that in the case of a complex reflection factor, the acoustic pressure is no longer maximum at the boundary.

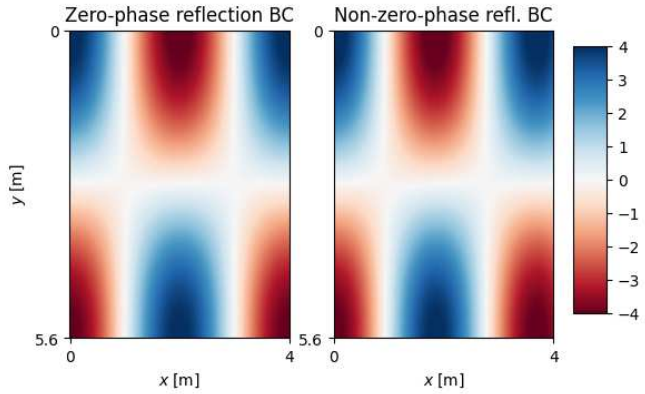

Fig. 5 Mode shape (pressure oscillation amplitude) for two similar modes with different boundary conditions. Both cases share the same pressure reflection factor amplitude at the boundary $x = L_x$, but they are phase-shifted by $\pi/3$.

An important advantage of the proposed approach is the possibility to use frequency-dependent boundary conditions. Fig. 6 shows the results for a 1D case with two variants of boundary conditions. Both variants assume $\zeta_{0x} = 10^3$. The first (blue) variant implements a simple Helmholtz resonator (HR) complex impedance boundary condition calculated as:

$$z_s = 0.2z_c + \mathrm{i}[2.371\omega - z_c \cot(0.2\omega/c)] \tag{20}$$

whereas the second (orange) variant uses the mean absolute value of the first one.

This choice is inspired by the HR surface acoustic impedance formulation proposed in [14]:

$$z_s = r_m + \mathrm{i}[\omega m - z_c \cot(kd)] \tag{21}$$

The results show that incorporation of a Helmholtz resonator can shift the room modes around their resonant frequency compared to the rigid boundary situation. This effect is more pronounced the closer they are to the Helmholtz resonance frequency. Secondly, the complex and frequency-dependent boundary conditions complicate the prediction of modes in multidimensional cases.

DOI 10.13164/juniorstav.2024.24121

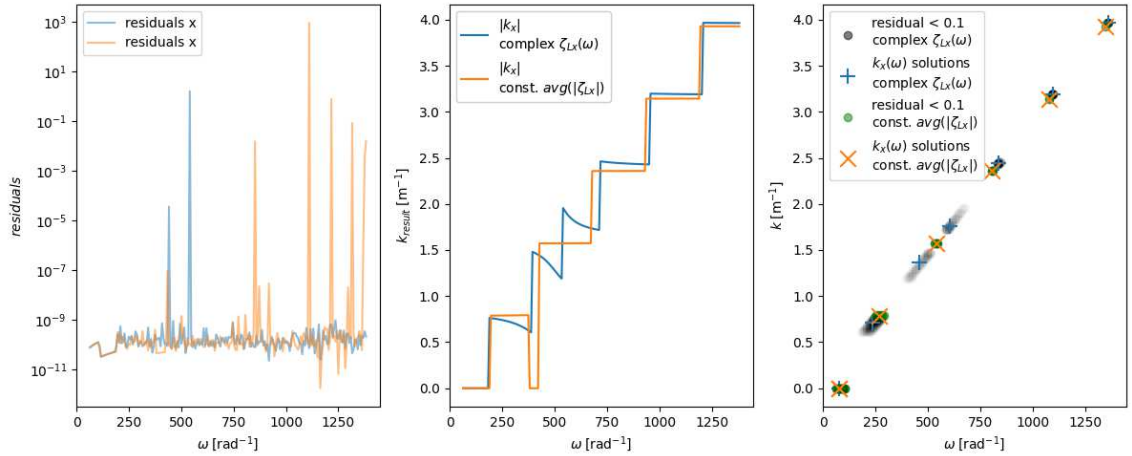

Fig. 6 Comparison between a frequency-dependent impedance boundary condition (blue) and a constant real-valued impedance boundary condition (orange) in terms of resulting possible wavenumbers in 1D. The two left panels are similar to those in Fig. 3, showing the minimization results for each angular frequency. The right panel illustrates the local minima regions for frequency-dependent (grey dots) and independent (green dots) impedance boundary conditions, as well as the respective minima positions denoted by blue and orange crosses.

4 DISCUSSION

This contribution extends the solution for symmetrical boundary conditions in a rectangular room mode frequency and wavenumber calculation described in [10] towards non-symmetrical and frequency-dependent boundary conditions. It presents several examples to demonstrate the current state of the proposed solution and its limitations.

First, several explicit solutions were derived for special cases. They met the expected behaviour with both real-valued and complex boundary conditions, some of which (the symmetrical cases) can also be found in [10].

Next (Fig. 1), the iterative approach was tested in 1D with several different constant impedance boundary conditions applied to one of the surfaces. These varied in the imaginary part and showed that (i) a non-zero phase of the impedance leads to shifts in mode frequency, (ii) the solution oscillates around one of the two real-valued solutions depending on the amplitude of the impedance and (iii) the minimization does not reveal the exact solution for Eq. (1) since it allows real-valued angular frequencies only. The latter is currently one of the main limitations to be resolved in future work.

The examples in Fig. 2, Fig. 3 and Fig. 4 extended the solution to 2D, still for frequency-independent boundary conditions. The possible wavenumber values were derived from the solution for axial modes in each direction. Based on these sets of values and angular frequency, a local minimum search was performed on the three-dimensional grid of values calculated via Eq. (18). The local minima were isolated based on an absolute threshold. The approach works well for simple cases. However, the threshold for identifying a minimum needed to be adjusted for each case manually to prevent skipping or merging any of the minima. This significantly limits the current robustness and first-derivative sign-based minimum identification algorithms should be adopted to improve the overall performance of the method.

The last example (Fig. 5) showed the mode search in 1D for the frequency-dependent complex boundary condition in the form of a Helmholtz resonator. The results reveal that a Helmholtz resonator can cause modal redistribution around its resonant frequency, in some special cases causing mode splitting. Besides this finding, the results uncovered several challenges to be overcome to make this approach usable. First, the search for wavenumbers resulting from the complex frequency-dependent boundary is complicated and frequency-dependent, which makes it impossible to extract a small subset of values. Instead, the whole solution needs to be considered. Second, related, it is also challenging to extend the frequency-dependent solution to more dimensions. Since the impedance depends implicitly on k, rather than on k_x, k_y or k_z, the solution does not consist of a choice from independent sets of values. From this perspective, a further improved minimization approach seems to be more suitable than a grid search.

DOI 10.13164/juniorstav.2024.24121

5 CONCLUSION

In this contribution, we extended the analytical solution of room mode calculation towards asymmetrical and frequency-dependent boundary conditions on the surfaces of a rectangular room. Even though the solution is not complete and we showed only some key examples, some conclusions can be made:

- Complex impedance boundary conditions shift the mode frequency solution around the real-valued boundary condition equivalent solution based on their amplitude. This is equivalent to an effective change in room dimensions.
- The minimization approach applied does not reveal an exact solution because the angular frequency was limited to real values (zero imaginary part).
- The grid search approach can be used to reveal modes in multidimentional cases but only restricted to frequency-independent boundary conditions. The absolute threshold local minima search does not seem to be robust for this application and should be improved.
- Frequency-dependent boundary conditions complicate the solution predominantly in multidimentional cases, where it is not simply possible to find a solution for wavenumber in one direction independent on the other.

Overall, the approach gives a satisfactory overview of possibilities and challenges related to minimization-based search for room modes in a rectangular room with complex impedance boundary conditions applied. Further research should focus on the search for an exact solution and frequency-dependent complex impedance boundary conditions applied in more than one dimension.

Acknowledgement

The contribution was produced with support for specific university research at Brno University of Technology, FAST- J-22-7880 (2022) and FAST-J-23-8284 (2023).

References

[1] FUCHS, Helmut V. and ZHA, Xueqin. Requirement for low-frequency reverberation in spaces for music: Part 1: Smaller rooms for different uses. *Psychomusicology: Music, Mind and Brain* [online]. September 2015. Vol. 25, no. 3, pp. 272–281. [Accessed 1 December 2022]. DOI 10.1037/pmu0000088

[2] SABINE, Wallace Clement. *Collected papers on acoustics.* Cambridge : Harvard University Press, 1922.

[3] SCHRÖDER, Dirk and VORLAENDER, Michael. RAVEN: A real-time framework for the Auralization of interactive virtual environments. In : *Proceedings of Forum Acusticum.* [online]. Aalborg, Denmark : European Acoustics Association, 2011. pp. 1541–1546. ISBN 978-84-694-1520-7.

[4] RINDEL, Jens and CHRISTENSEN, Claus. ODEON, A DESIGN TOOL FOR NOISE CONTROL IN INDOOR ENVIRONMENTS. In : *Noise at Work*. [online]. Lille, France, 3 July 2007. p. 9. [Accessed 11 November 2022]. Available from: https://www.researchgate.net/publication/251795869_ODEON_A_DESIGN_TOOL_FOR_NOISE_CONTROL_IN_INDOOR_ENVIRONMENTS

[5] Enabling a better sounding world [online].Treble. 2024 Treble Technologies ehf. [Accessed 25 October 2023]. Available from: https://www.treble.tech/

[6] ARETZ, Marc, NÖTHEN, René, VORLAENDER, Michael and SCHRÖDER, Dirk. Combined Broadband Impulse Responses Using FEM and Hybrid Ray-Based Methods. In : *Proceedings of the EAA Auralization Symposium.* [online]. Espoo, Finland, June 2009. p. 6. Available from: https://www.researchgate.net/publication/258098666_Combined_Broadband_Impulse_Responses_Using_FEM_and_Hybrid_Ray-Based_Methods

[7] KRITLY, Leopold, SLUYTS, Yannick, PELEGRÍN-GARCÍA, David, GLORIEUX, Christ and RYCHTARIKOVA, Monika. Discrimination of 2D wall textures by passive echolocation for different reflected-to-direct level difference configurations. *PLOS ONE* [online]. 27 May 2021. Vol. 16, p. e0251397. DOI 10.1371/journal.pone.0251397

[8] SHTREPI, Louena, ASTOLFI, Arianna, PUGLISI, Giuseppina Emma and MASOERO, Marco Carlo. Effects of the Distance from a Diffusive Surface on the Objective and Perceptual Evaluation of the Sound Field in a Small Simulated Variable-Acoustics Hall. *Applied Sciences* [online]. March 2017. Vol. 7, no. 3, p. 224. [Accessed 31 October 2023]. DOI 10.3390/app7030224

[9] KRIZ, J., PORCINAI, E., LEPA, S. and WEINZIERL, S. Effect of Early Reflections on Stage Acoustic

Conditions for Solo Musicians. In : *Proceedings of the 10th Convention of the European Acoustics Association Forum Acusticum 2023*. [online]. Turin, Italy : European Acoustics Association, 17 January 2024. p. 3933–3940. [Accessed 26 March 2024]. ISBN 978-88-88942-67-4. DOI 10.61782/fa.2023.0113.

[10] KUTTRUFF, Heinrich. *Room acoustics* [online] . 4th ed. London, New York, NY : Spon Press, 2000. ISBN 978-0-419-24580-3

[11] NELDER, J. A. and MEAD, R. A Simplex Method for Function Minimization. *The Computer Journal* [online]. 1 January 1965. Vol. 7, no. 4, p. 308–313. [Accessed 26 October 2023]. DOI 10.1093/comjnl/7.4.308

[12] VIRTANEN, Pauli, GOMMERS, Ralf, OLIPHANT, Travis E., HABERLAND, Matt, REDDY, Tyler, et al. SciPy 1.0: fundamental algorithms for scientific computing in Python. *Nature Methods* [online]. 2020. Vol. 17, no. 3, pp. 261–272. DOI 10.1038/s41592-019-0686-2

[13] GAO, Fuchang and HAN, Lixing. Implementing the Nelder-Mead simplex algorithm with adaptive parameters. *Computational Optimization and Applications* [online]. 1 January 2012. Vol. 51, no. 1, p. 259–277. [Accessed 26 October 2023]. DOI 10.1007/s10589-010-9329-3

[14] COX, Trevor J. and D'ANTONIO, Peter. *Acoustic absorbers and diffusers: Theory, design and application*. 3rd ed. Taylor, 2017. ISBN 978-0-415-47174-9